The assessment of surface areas in porous carbons by two model-independent techniques, the DR equation and DFT

T.A. Centeno[a], F. Stoeckli[b,*]

[a]Instituto Nacional del Carbon-CSIC, Apartado 73, E-33080 Oviedo, Spain

[b]Institut de Physique de l'Université, Bellevaux 51, CH-2000 Neuchâtel, Switzerland

ABSTRACT

The strong linear correlation observed between S_{BET} and the micropore volume of 190 carbons with pore widths between 0.5 and 1.8 nm confirms the unreliable character of S_{BET}, in spite of its frequent use. (It corresponds approximately to 2200-2300 m^2 per cm^3 of micropores, whatever their width). Alternative determinations of the surface area are therefore required. It is shown that two model-independent techniques (Kaneko's comparison plot for nitrogen and the enthalpies of immersion into aqueous solutions of phenol) and two model-dependent approaches (Dubinin's theory and DFT) lead to total surface areas which are in good agreement. Their average S_{av} is probably a reliable assessment of the total surface area. It is often in disagreement with S_{BET}, but a closer study of 42 well characterized microporous carbons, for which all four techniques are available, shows that the ratio S_{BET}/S_{av} increases linearly with the average pore width. This should be taken into consideration when surface-related properties (*e.g.* densities of chemical groups or adsorbed species, specific capacitances) are examined on the basis of a single determination and in particular on the BET technique.

---

*Corresponding author: Fax: +41 32 7182511. E-mail address: fritz.stoeckli@unine.ch (F. Stoeckli)

1. Introduction and general background

The reliable assessment of surface areas in porous carbons is of great relevance in the study of specific properties, for example the surface density of chemical species or electrochemical double layer capacitances (EDLC). Sophisticated approaches such as the density functional theory (DFT) and its successive developments (NLDFT, QSDFT) [1-6], as well as the simple BET theory [7-10] are commonly used, but frequently on their own and without reference to other techniques. Comparisons would provide an estimate of the reliability of the corresponding surface-related properties. It appears that there may be important differences, in particular between the BET model and practically all other determinations, except for nanopores around 0.9 nm. This can lead to diverging interpretations of surface related properties. Moreover, a number of recent studies dealing with EDLC properties [11-13] combine the density functional approach and BET, although they are based on completely different models. The average pore size is derived from the former and the latter provides the specific area S_{BET}, although the areas S_{DFT} and S_{BET} are often different.

The possibilities of both models are known and in particular the limitations of the BET approach have been pointed out, for example, by K. Sing [8], F. Rouquérol *et al.* [9] and more recently by J. Rouquérol *et al.* [10]. The IUPAC recommendations of 1985 [14] and 1994 [15] also state that in the case of microporous solids the values of surface areas derived from either the Langmuir or the BET analysis are incorrect. Therefore, it is recommended to refer to the *equivalent* BET-nitrogen surface area of the solid. Obviously, this does not imply that it actually corresponds to the surface area of an activated carbon, which consists of the micropore walls S_{mi} and the external area S_e.

This means that further interpretations based on S_{BET} may be misleading.

It appears that for typical micropores (or nanopores, as they are frequently called since the mid-1990s), the BET analysis often overestimates the total surface area with respect to other determinations, as illustrated for example by Shi [16]. This has also been reported quantitatively by Thomson and Gubbins [17] who used reverse Monte Carlo modeling. They showed that the analysis of a nitrogen isotherm generated for a nanoporous carbon with a nominal area of 1070 m^2 g^{-1} leads to a BET surface area S_{BET} of 1510 m^2 g^{-1}. Ustinov *et al.* [5] report a similar pattern for four samples of strongly activated carbons analyzed by an improved NDLFT approach. They also show the effect of different versions of NLDFT on the pore size distribution of a given carbon. On the basis of their work with the Hybrid Reverse Monte Carlo technique, Palmer *et al.* [18] also expressed their reservations about the reliability of the BET surface area. Similar conclusions can be drawn from the analysis of the surface areas for pore size distributions generated by Monte Carlo modeling based on slit-shaped nanopores.

The validity of the BET equation for the characterization of microporous adsorbents has also been addressed recently and in detail by J. Rouquérol *et al.* [10]. This follows an earlier paper [9] dealing with the texture of porous materials and the authors point out the precautions which must be taken in the BET analysis. It is therefore surprising that other approaches have not been used more systematically in order to cross-check results based on the BET analysis and eliminate possible contradictions.

Furthermore, as discussed in detail below (section 3), a comparison of S_{BET} with the micropore volume of carbons V_{mi} reported by different authors [19-28] and including our own data, shows that the two are strongly correlated. For 190 carbons, which cover practically the entire range of microporosity (0.5 to 1.8 nm), the linear correlation leads to an average of 2300 m^2 cm^{-3} for the ratio S_{BET}/V_{mi}. This suggests, to a first and good

approximation, that the average width of the locally slit-shaped pores should be around 0.9 nm for all the carbons, which is in contradiction with the actual dimensions determined by different techniques. The micropore volumes, derived mainly from Dubinin's theory and from the NLDFT model, may be regarded as reliable, although they are slightly different. Therefore, one may assume that the above geometrical paradox is probably related to S_{BET} and its validity may be questioned.

We wish to illustrate the relevance of using several independent assessments of the total surface area of porous carbons and in particular of their average S_{av}. The latter probably corresponds to a reliable assessment of the total surface area available to small adsorbates in microporous carbons. It will be shown, for example, that the ratio S_{BET}/S_{av} is a linear function of the average pore width between 0.66 and 1.65 nm, which offers a quantitative explanation for conflicting results found in the literature.

The present study is based on the nitrogen comparison plot [7-9, 29-31] and on immersion calorimetry in aqueous solutions of phenol [32-35]. The latter approach is also supported by studies of phenol adsorption at the liquid-solid interface, showing that it is limited to a single layer on the micropore walls and on the outside. These are model-free approaches which provide direct and coherent information on the surface area accessible to small molecules. Furthermore, the surface areas obtained from these techniques are also in good agreement with the predictions of the Dubinin-Radushkevich equation [7, 36-37], supported by Monte Carlo simulations. It would therefore be reasonable to combine these approaches in order to obtain a reliable assessment of surface areas, rather than to rely on a single determination.

The surface areas S_{DFT} based on the density functional theory (mainly the NLDFT version found in current software packages) are also examined here, but it appears that they show some scatter with respect to the other determinations.

1.1. The comparison plot (SPE technique)

The development of Sing's α_S comparison plot [7] by Kaneko *et al.* [29-31], the so-called SPE technique (subtracting pore effect), allows the determination of the total surface area S_{comp} and the external surface area S_e of porous carbons, by using the nitrogen adsorption isotherm at 77 K. The two surface areas correspond, respectively, to the slopes of the initial and the final sections of the plot. It follows that the surface area of the micropore walls, S_{mi}, corresponds to the difference (S_{comp} - S_e). For the model of locally slit-shaped pores, the average width w (nm) is

$$w = 2000\ V_o / (S_{comp} - S_e), \qquad (1)$$

where V_o represents the volume of the micropores filled by liquid-like nitrogen. It is either $V_{o,s}$ obtained from the extrapolation of the second linear section of the plot, or the micropore volume W_o obtained from the DR analysis (section 1.3). The two are usually in good agreement (see for example Table 1 in ref. [31]).

The SPE technique is limited to pore sizes above 0.6 to 0.7 nm, in particular due to the absence of a clear linear range. The comparison with Monte Carlo modeling of nitrogen adsorption [30] also indicates that in narrow pores (w < 1.1 nm), S_{comp} overrates the effective surface area by a factor of up to 15 percent which must be taken into account. This increase in adsorption reflects the enhancement of the gas-solid energy in narrow pores, compared to open surfaces, but the effect rapidly decreases.

Our approach is basically the same as the classical α_S plot method, but we use a direct comparison of the N_2 (77 K) isotherm with the standard isotherm for *Vulcan 3* given by Rouquerol *et al.* [9]. Comparison plots can also be obtained for other

adsorbates and reference isotherms have been provided, for example, by Carrott *et al.* for C_6H_6 [38] and CH_2Cl_2 [39]. As shown in Table 1, the results including isolated data for CO_2 and CCl_4, are in good agreement with those of N_2.

1.2. Immersion calorimetry

This model-free technique is based on the selective adsorption of phenol from dilute aqueous solutions (*e.g.* 0.4M) onto carbons [32-35]. Under these conditions, as indicated by the analysis of the type I solid-liquid isotherm [34, 35], phenol forms only a monolayer on both the walls of the micropores and on the external surface area S_e. Moreover, the corresponding areas are in good agreement with other determinations. (Note that the micropore volume is filled by phenol only if it is adsorbed from the vapour phase or by immersion into phenol fluidized by 15-20 per cent w/w of water, as described in detail elsewhere [33]). Adsorption of phenol from the dilute solution can also be monitored by immersion calorimetry, which is less tedious than the determination of solid-liquid isotherms. For typical graphitized carbon blacks of known surface areas (*e.g. N234-G*, *Hoechst, Vulcan 3*) the process corresponds to an average value of $-(0.105 \pm 0.004)$ J m^{-2} [34]. It will be shown that in the case of porous carbons the enthalpies of immersion lead to total surface area S_{phenol} which are in good agreement with the other determinations.

1.3. The Dubinin-Radushkevich equation

For nanoporous carbons, the adsorption isotherm of nitrogen (or other small molecules) can also be analyzed by Dubinin's theory for the volume filling of micropores [7,36,37]. The linearization of the Dubinin-Radushkevich equation leads to the micropore volume

W_o and the so-called characteristic energy E_o of the carbon. The latter is related to the average width L_o of locally slit-shaped micropores by

$$L_o\ (nm) = 10.8/(E_o - 11.4\ kJ\ mol^{-1}) \quad (2)$$

This expression relies on different techniques [40], but it can be obtained directly by Monte Carlo simulations of pore size distributions for CO_2 (273 K) and C_6H_6 (293 K) adsorbed in slit-shaped pores. It was further verified by Ohba's Monte Carlo modeling of N_2(77 K) for pores of 1 and 1.2 nm [41].

By symmetry with Eq.(1), one obtains the surface area of the micropore walls

$$S_{mi}(DR)\ (nm) = 2000W_o(cm^3\ g^{-1})/L_o(nm) \quad (3)$$

and the total surface area $S_{tot}(DR)$ is

$$S_{tot}(DR) = S_{mi}(DR) + S_e\ . \quad (4)$$

Eq.(4) was used for the nitrogen isotherms determined at 77 K and, as shown in Table 1, similar results were obtained for other small adsorbates.

Unlike S_{comp} and S_{phenol}, $S_{tot}(DR)$ is model-dependent (slit-shaped pores), but it appears that these areas are usually in good agreement (see below).

1.4. Density functional theory

Nowadays the density functional theory (DFT) plays a major role in the characterization of porous carbons. Consequently, this approach must also be

addressed here, as far as the determination of surface areas is concerned. An excellent presentation of the state of the art can be found in the work of Neimark *et al.* [2-3] and in their recent review [6]. Therefore, we limit ourselves to the essential features. The NLDFT model used for N_2 at 77 K is provided in standard packages and it is featured in a recent ISO standard [42]. It considers homogeneous slit-shaped pores, but unlike the Monte Carlo approach, its pore size distribution suffers from a false gap in the region of 1 nm. This feature, which may introduce some uncertainty in the cumulative surface area S_{DFT} and the micropore volume, has been corrected in the recent QSLDFT development [6]. As far as the pore size distributions are concerned, the compatibility between DFT and other approaches such as GCMC (Grand Canonical Monte Carlo), SPE and DR has been examined by different authors*, e.g.* [1-6, 41, 43]. However, a systematic comparison of NLDFT and in particular of QSLDFT-based surface areas with other determinations is still lacking.

2. Experimental

The study is based on 48 carbons obtained from a variety of precursors (lignocellulosic, polymers and metal carbides). Forty six samples are microporous and two templated carbons are exclusively mesoporous with pore diameters centered at 5.1 and 9.3 nm. Details can be found in refs. [36,37,44-46]. As shown by TPD (Thermally Programmed Desorption) and the enthalpies of immersion into water, the surface density of oxygen atoms is below 3 μmol m^{-2} or less than 20 per cent of S_{tot}.

The adsorption of N_2 (77 K) was determined with a *Micromeritics ASAP 2010* apparatus and the data was analyzed with the help of its software package, leading to BET and NLDFT areas. On the other hand, the micropore volumes W_o and the average pore widths L_o were determined by using Dubinin's theory [7,36,37,45].

The data for S_{BET} was obtained by selecting in each case the best linear fit of the corresponding plot following the criteria listed by J. Rouquerol *et al.* [10] for the BET analysis in the case of microporous carbons. As indicated by these authors, the linear range is found below the classical domain of p/p_o between 0.05 and 0.3. This is illustrated by the example of six carbons covering the range of microporosity between 0.68 and 2.1 nm. As shown in Table S1 of the supplementary data provided with this paper (Appendix A), when the average micropore size L_o decreases from 2.1 nm (PX-21) to 0.68 nm (HK-650-8), the linear range shifts from respectively 0.049-0.216 to 0.0009-0.081. At the same time, constant c_{BET} increases from 72 to 35476, clearly reflecting the higher adsorption energy in the smaller pores. The influence of microporosity on adsorption is also reflected by the semi-logarithmic plot of the isotherms of the six carbons. Further and quantitative information is obtained from the DR analysis.

It may be assumed that the data reported in the literature and obtained by similar software packages satisfies these criteria. On the other hand, no details are known about the NLDFT calculations.

The comparison plots for nitrogen were based on the data for *Vulcan-3* (80 $m^2\ g^{-1}$) [9] and the correction of 15% [29] has been applied to pores below 1.1 nm. In some cases the plot was cross-checked by our own reference isotherm on graphitized carbon black *Hoechst* (52 $m^2\ g^{-1}$), which leads to similar results. Separate experiments were also carried out for a number of samples, using mainly CH_2Cl_2 and C_6H_6 vapours at 293-298 K in a classical gravimetric apparatus of the McBaine type [7]. The reference isotherms based on carbon *Hoechst* gave results which are in good agreement with the data of the corresponding nitrogen plots. Typical examples of comparison plots of carbons of the present series are shown elsewhere [46,47].

Immersion calorimetry was carried out with four identical calorimeters of the Tian-Calvet type, specifically designed for work with carbons and measuring absolute energies between 2 to 20 Joules [44]. Typically, 0.025 to 0.080 g were outgassed at 10^{-5} Torr for 6 to 10 hours below 400-450 K, and subsequently immersed at 293 K into 5 ml of aqueous solutions of phenol (0.4 M). The calorimeters were calibrated electrically and cross-checked by the dissolution of dry KNO_3 into de-ionized water (345 J g^{-1}). The reproducibility of the enthalpies of immersion $\Delta_i H$ for homogeneous samples is within 2-3 per cent.

For the study of the correlation between S_{BET} and the micropore volume V_{mi}, we added two sets of respectively 16 and 10 carbons from our laboratory, but with a less exhaustive characterization than the basic set of this study. We also used 10 sets of data reported in the literature and dealing with specific types of carbons [13,19-28] (see Table 2). Their total amounts to 122 carbons.

It should be pointed out that some authors characterize their solids with argon and use the corresponding software to determine BET areas and volumes. However, this adsorbate leads to the same results as nitrogen at 77 K, used in the present study.

3. Results and discussion

3.1. BET analysis

As shown in Fig. 1 and in agreement with earlier observations [46], there exists a strong linear correlation between the values of S_{BET} and V_{mi} for the 68 samples from our laboratory and the 122 carbons reported by different authors [13,19-28]. The volume V_{mi} is either W_o or, in the case of [13,23,24,28], the value obtained from the NLDFT analysis. The data covers the range of 173 m^2 g^{-1} < S_{BET} < 3290 m^2 g^{-1} and 0.08 cm^3 g^{-1}< V_{mi}< 1.45 cm^3 g^{-1}, with pore sizes between 0.5 nm and 1.8 nm. The overall linear

correlation for the 190 carbons is

$$S_{BET} = (2300 \pm 20\ m^2\ cm^{-3}) \cdot V_{mi} \quad (5)$$

and the uncertainty corresponds to the standard deviation, σ.

A closer examination of the data (see Table 2) suggests no significant trends for the ratios S_{BET}/V_{mi} within any individual series of carbons. This is illustrated by Fig. 2, which shows as examples distinct series, namely CO_2 activated fibers [22], TiC-based CDCs treated with H_2, or activated with KOH and CO_2 [28] and a group of 24 carbons obtained by chemical (KOH, NaOH) and physical (CO_2, H_2O) activation [25]. These series of carbons cover practically the entire range of microporosity.

Although the corresponding pore sizes are not provided in some reports, it is well known that that activation to high burn-offs leads to a widening of the pores. This is certainly the case, for example, for the extensive work of Bleda-Martinez *et al.* [25] and Lozano-Castello *et al.* [27], where the ratios S_{BET}/V_{mi} are remarkably constant (respectively, 2220 ± 120 $m^2\ cm^{-3}$ and 2190 ± 80 $m^2\ cm^{-3}$ for different series of 24 and 14 activated carbons).

In some cases [19-21] including our carbons, the data for S_e is also available and it is possible to calculate surface area $S_{BET} - S_e$ associated exclusively with the micropores. The above analysis can be refined by examining the ratios $(S_{BET} - S_e)/V_{mi}$. The average values (see Table 2) are somewhat lower and provide an estimate of the corresponding width of slit-shaped micropores, $w = 2000V_{mi}/(S_{BET} - S_e)$. It is around 0.85-0.9 nm for all carbons and in clear contradiction with the values obtained by different techniques, such as the adsorption of molecules of different sizes, immersion calorimetry, the DR equation and DFT-based analysis. If one assumes that these determinations and the

values of W_o are relatively accurate, it follows that neither $S_{BET} - S_e$ nor S_{BET} can be associated directly with the micropore area S_{mi} or the total surface area S_{tot} of the carbons. The only exceptions would be carbons with average pore widths L_o around 0.9 nm. It is also interesting to point out that the monolayer equivalent of 1 cm^3 of liquid nitrogen at 77 K is 2814 m^2.

The foregoing observations alone challenge the systematic and often exclusive use of S_{BET} to derive surface related properties as reported, for example, in electrochemistry [11-13], in studies of hydrogen storage [22, 28, 48] or the amounts of oxygen-containing groups [25]. Furthermore, pores of less than 0.8 to 0.9 nm can no longer accommodate two layers of nitrogen or argon and S_{BET} inevitably underestimates the surface of their walls. One may therefore expect that the comparison plot, as well as the other converging approaches examined here, will provide a more reliable estimate of the surface area available to small molecules or ions, than S_{BET}.

3.2. Immersion calorimetry and comparison plot

As shown in Fig. 3, the 48 untreated micro- and mesoporous carbons reveal a good correlation between the enthalpy of immersion $\Delta_i H$(phenol 0.4 M) and the total surface area $S_{comp}(N_2; 77K)$. The linear correlation is

$$\Delta_i H(\text{phenol 0.4M})\ (\text{J g}^{-1}) = -\ (0.105 \pm 0.002)\ (\text{J m}^{-2})\ S_{comp}(N_2; 77K)\ (\text{m}^2\ \text{g}^{-1}) \qquad (6)$$

The factor -(0.105 ± 0.002) J m^{-2} is the same as the average value of -(0.105 ± 0.004) J m^{-2} obtained for three different carbon blacks [34]. This suggests that $\Delta_i H$ can be used to determine independently a total surface area $S_{phenol} = -\Delta_i H$(phenol 0.4M) J g^{-1}/0.105 J m^{-2} of microporous carbons, accessible to small probes. Moreover, it appears that for

carbons with low oxygen contents the surface area based on -0.105 J m^{-2} is in good agreement with the value derived from the limiting adsorption of phenol from aqueous solutions, assuming a molecular area of $45 \cdot 10^{-20}$ m^2 (or 270 m^2 $mmol^{-1}$) [34]. As pointed out earlier [34], water shows a strong affinity for oxygen-containing complexes, which reduces the adsorption of phenol. For the present carbons, the oxygen density $[O]_{TPD}$ is below 3 μmol m^{-2}, or less than 20 per cent of S_{tot} if all the sites are saturated by water. Moreover, due to a compensating effect in the energies, the overall enthalpy remains practically constant, which justifies the use of Eq.(6). However, high enthalpies of immersion can be observed for carbons subjected to chemical treatments and for certain fibers. These enthalpies probably reflect surface reactions involving phenol, which means that it is recommended to compare systematically S_{phenol} with $S_{comp}(N_2\ 77K)$.

3.3. Comparison plot and DR analysis

Fig. 4 shows a good linear correlation (1.01 ± 0.01) between S_{tot}(DR) based on nitrogen and $S_{comp}(N_2; 77K)$ for the 42 nanoporous carbons with 0.66 nm < L_o < 1.65 nm, where the DR approach is valid. The good correlation is not too surprising, since S_{mi}(DR) is based on Monte Carlo modeling in slit-shaped micropores and the micropore area of Kaneko's SPE method, S_{comp}- S_e, has been verified by the same theoretical approach [30,41]. It is therefore not surprising to find an equally good correlation between $-\Delta_i H$(phenol 0.4M) and S_{tot}(DR). On the other hand, S_{phenol}, S_{tot}(DR) and S_{comp} show no direct correlations with S_{BET}, but an alternative explanation is provided below.

3.4. Average total surface area S_{av} and S_{BET}

It appears that the two model-free areas, S_{comp} and S_{phenol}, and the area $S_{tot}(DR)$ based on the model of locally slit-shaped nanopores, are in good agreement. This means that their average $S_{av}(3) = [S_{comp} + S_{phenol} + S_{tot}(DR)]/3$ should provide a reliable assessment of the total surface area accessible to small molecules and ions in nanoporous carbons. On the other hand, S_{BET} can show significant deviations from $S_{av}(3)$. The difference between the two is revealed by the variation of the ratio $S_{BET}/S_{av}(3)$ of the 42 nanoporous carbons with the average width L_o. The linear correlation

$$S_{BET}/S_{av}(3) = (1.20 \pm 0.02)\, L_o \qquad (7)$$

shown in Fig. 5 is valid in the range 0.6 to 1.7 nm and provides a clear quantification of the deviations (or the variable agreements) reported in the literature.

It appears that all determinations converge for pores around 0.85 nm, where two layers of nitrogen can be accommodated in the locally slit-shaped micropores. Below this value, S_{BET} becomes inevitably smaller than the effective area of the walls. On the other hand, for pores above 0.85 nm, S_{BET} gradually diverges and at widths around 1.8 nm it corresponds to more than twice the average of the other determinations. Beyond 2 to 3 nm, *i.e.* in mesopores, the ratios S_{BET}/S_{comp} and S_{BET}/S_{phenol} decrease and finally converge for open surfaces. This means that with respect to $S_{av}(3)$ or an average area including other independent determinations such as $S_{comp}(CO_2)$, $S_{comp}(CH_2Cl_2)$ and $S_{comp}(C_6H_6)$ (see Table 1), S_{BET} overrates surface related properties for pores below 0.85 nm. On the other hand, it gradually underrates them in wider pores. This should be kept in mind when trying to transform reliable gravimetric properties such as mmol g^{-1} [22,25,28,48] or F g^{-1} [11-13] into surface related properties (mmol m^{-2} for chemical

species or atoms and F m^{-2} for EDLC). The *statistical* correction factor to be applied to S_{BET} and leading to an estimate of the probable total surface area is provided by Eq.(7).

3.5. Average surface area including S_{DFT}

As mentioned in section 1.4, the density functional theory and its successive developments play a major role in the routine assessment of surface areas of porous carbons. Therefore, this approach must also be addressed here by examining the use of S_{DFT} obtained by the NLDFT analysis.

As seen in Fig. 5, the average total surface area $S_{av}(4) = [S_{comp} + S_{phenol} + S_{tot}(DR) + S_{DFT}]/4$ obtained for our 42 microporous carbons leads to a linear correlation between $S_{BET}/S_{av}(4)$ similar to that observed with $S_{av}(3)$. The slope is practically the same, with a slightly larger standard deviation (1.19 ± 0.03) nm^{-1}. This is not too surprising in view of the uncertainty related to the dip in the PSD around 1 nm. For carbons with narrow pores (L_o < 1.1 nm), where uncertainties may arise, the correlation leads to (1.14 ± 0.02) nm^{-1}, which confirms the general pattern.

The divergences observed between S_{DFT} and S_{BET} may have led a number of authors to prefer intuitively the latter, but Eq. (7) shows that it was probably not the best choice.

Regarding the differences between S_{DFT} and the other determinations, S_{comp}, S_{phenol} and $S_{tot}(DR)$, it is likely that the recent QSDFT approach (Quenched Solid Density Functional Theory) will lead to a better agreement. It takes into account surface geometrical inhomogeneity and suppresses the artificial gap in the PSD around 1 nm. Unfortunately, no systematic comparison of the areas S_{QSDFT} with those obtained by other techniques seems to be available yet.

At this stage it is possible, with the help of Eq.(7), to make a clear distinction between the predictions of the total surface area accessible to small molecules, based on the one hand on the average of different determinations and, on the other hand, the BET analysis. For example, the recent use of S_{tot}(DR) [41] and S_{av}(3) [50,51] already suggested that surface-related EDLC properties are relatively independent of the average pores size as opposed to the approach based on S_{BET} [11-13].

The present study is only a first step in the assessment of surface areas available in carbons, since the accessibility to larger molecules or ions depends on both the pore size distribution and the presence of constrictions. Under these circumstances further techniques must be considered, such as the determination of reliable PSDs and their cumulative surface areas, or the use of comparison plots of larger molecules such as CCl_4. In this context, variable preadsorption and immersion calorimetry into liquids of increasing molecular dimensions [36] play an important role. Work is currently in progress along these lines and results will be published in due course.

4. Conclusions

The analysis of data for 190 carbons with micropore widths between 0.5 and 1.8 nm shows that the BET surface area is closely related to the micropore volume V_{mi} and suggests an area of approximately 2200-2300 m^2 cm^{-3}, whatever the actual pore width. (By comparison, the monolayer equivalent to 1 cm^3 of liquid nitrogen at 77 K is 2814 m^2). This general correlation is confirmed within series of carbons of similar origins and treatments. It follows that S_{BET} can be representative only for carbons with pore widths around 0.9 nm, if one assumes the model of locally slit-shaped pores. Other techniques

must therefore be considered to provide a reliable assessment of their total surface area.

We show that for 42 microporous carbons (pore widths 0.66 nm $<L_o<$ 1.65 nm) the combination of the nitrogen comparison plot (Kaneko's SPE method), the enthalpy of immersion into aqueous solutions of phenol, the Dubinin-Radushkevich equation and the DFT approach lead to an average surface area S_{av} which probably corresponds to a good estimate of S_{tot} for microporous carbons. The BET area diverges from it as expressed quantitatively by Eq. (7) and the two values are similar only for pore widths around 0.9 nm. This implies that the calculation of surface-related properties based on S_{BET} alone can be misleading and a better estimate requires the correction factor implied by Eq. (7).

The present results apply essentially to small molecules or ions and in the case of larger adsorbates the pore size distribution and constrictions can reduce significantly their accessibility. This means that surface areas determined with the help of nitrogen or argon may loose their meaning and the present techniques must be adapted in order to provide a reliable assessment of the surface area available to larger molecules.

References

[1] Lastokie C, Gubbins KE, Quirke N. Pore size distribution analysis of microporous carbons: a density functional theory approach. J Phys Chem 1993; 97(18): 4786-96.

[2] Ravikovitch PI, Vishniakov A, Russo R, Neimark AV. Unified approach to pore size characterization of microporous carbonaceous materials from N_2, Ar and CO_2 adsorption isotherms. Langmuir 2000; 16(5): 2311-20.

[3] Ravikovich PI, Neimark AV. Characterization of nanoporous materials from adsorption and desorption isotherms. Colloid Surface A 2001; 187-188: 11-21.

[4] Jagiello J, Thommes M. Comparison of DFT characterization methods based on N_2, Ar, CO_2 and H_2 adsorption applied to carbons with various pore size distributions. Carbon 2004; 42(7): 1227-32.

[5] Ustinov EA, Do DD, Fenelonov VB. Pore size distribution analysis of activated carbons: Application of density functional theory using nongraphitized carbon black as a reference system. Carbon 2006; 44(4): 653-63.

[6] Neimark AV, Lin Y, Ravikovitch PI, Thommes M. Quenched solid density functional theory and pore size analysis of micro-mesoporous carbons. Carbon 2009; 47(7): 1617-28.

[7] Gregg SJ, Sing KSW. Adsorption, surface area and porosity. Academic Press. New York 1982. p. 42, 94, 218, 257.

[8] Sing K. The use of nitrogen adsorption for the characterization of porous materials. Colloid Surface A 2001; 187-188: 3-9.

[9] Rouquérol F, Luciani L, Llewellyn Ph, Denoyel R, Rouquérol J. Texture des matériaux pulvérulents ou poreux, Editions Techniques de l'Ingénieur, Paris 2004, p. 1-24.

[10] Rouquérol J, Llewellyn P, Rouquérol F. Is the BET equation applicable to microporous adsorbents? In: Llewellyn P, Rodriguez-Reinoso F, Rouquérol J, Seaton N, editors. Studies in Surface Science and Catalysis 160. Elsevier. Amsterdam 2007. p. 49-56.

[11] Chmiola J, Yushin G, Gogotsi Y, Portet C, Simon P, Taberna PL. Anomalous increase in carbon capacitances at pore sizes less than 1 nm. Science 2006; 313:1760-3.

[12] Chmiola J, Yushin G, Dash R, Gogotsi Y. Effect of pore size and surface area of carbide derived carbons on specific capacitance. J Power Sources 2006; 158(1): 765-72.

[13] Largeot C, Portet C, Chmiola J, Taberna PL, Gogotsi Y, Simon P. J. A. Relation between the ion size and pore sizes for an electric double-layer capacitor. J Am Chem Soc 2008;130(9): 2730-1.

[14] Sing KSW, Everett DH, Haul RAW, Moscou L, Pierotti RA, Rouquérol J, Siemieniewska T. Reporting physisorption data for gas/solid systems. Pure Appl Chem 1985; 57(4): 603-19.

[15] Rouquérol J, Avnir D, Fairbridge CW, Everett DH, Haynes JH, Pernicone N, Ramsay JDF, Sing KSW, Unger KK. Recommendations for the characterization of porous solids. Pure Appl Chem 1994; 66(8): 1740-58.

[16] Shi H. Activated carbons and double layer capacitance. Electrochim Acta 1996; 41(10):1633-9.

[17] Thomson TK, Gubbins KE. Modeling structural morphology of microprous carbons by reverse Monte Carlo. Langmuir 2000; 16(13): 5761-73.

[18] Palmer JC, Brennan JK, Hurley MM, Balboa A, Gubbins KE. Detailed structural models for activated carbons from molecular simulation. Carbon 2009; 47(12): 2904-13.

[19] Gryglewicz G, Machnikowski J, Lorenc-Grabowska E, Lota G, Frackowiak E. Effect of pore size distribution of coal-based activated carbons on double layer capacitance. Electrochim Acta 2005; 50(5): 1197-1206

[20] Seredych M, Gierak A. Influence of water on adsorption of organic compounds from its aqueous solutions on surface of synthetic active carbons. Colloid Surface A 2004; 245(1-3): 61-7.

[21] Seredych MM, Gun'ko VM, Gierak A. Structural and energetic heterogeneities and adsorptive properties of synthetic carbon adsorbents. Appl Surf Sci 2005; 242(1-2): 154-161.

[22] Salvador F, Sánchez-Montero MJ, Montero J, Izquierdo C. Hydrogen storage in carbon fibers activated with supercritical CO_2: Models and the importance of porosity. J Power Sources 2009; 190(2): 331-5.

[23] Seredych M, Portet C, Gogotsi Y, Bandosz TJ. Nitrogen modified carbide-derived carbons as adsorbents of hydrogen sulfide. J Colloid Interf Sci 2009; 330(1): 60-6

[24] Jänes A, Thomberg T, Lust E. Synthesis and characterisation of nanoporous carbide-derived carbon by chlorination of vanadium carbide. Carbon 2007; 45(14): 2717-22

[25] Bleda-Martínez MJ, Maciá-Agulló JA, Lozano-Castelló D, Morallón E, Cazorla-Amorós D, Linares-Solano A. Role of surface chemistry on electric double layer capacitance of carbon materials. Carbon 2005; 43(13): 2677-84.

[26] Nian YR, Teng H. Influence of surface oxides on the impedance behavior of carbon-based electrochemical capacitors. J Electroanal. Chem. 2003; 540:119-27.

[27] Lozano-Castelló D, Lillo-Ródenas MA, Cazorla-Amorós D, Linares-Solano A. Preparation of activated carbons from Spanish anthracite: I. Activation by KOH. Carbon 2001; 39(5): 741-9.

[28] Gogotsi Yu, Portet C, Osswald S, Simmons JM, Yildirim T, Laudisio G, Fischer JE. Importance of pore size in high-pressure hydrogen storage by porous carbons. Int J Hydrogen Energ 2009; 34(15):6314-9.

[29] Setoyama N, Ruike M, Kasu T, Suzuki T, Kaneko K. Surface characterization of microporous solids with He adsorption and small angle X-ray scatering. Langmuir 1993; 9(10):2612-7.

[30] Setoyama N, Suzuki T, Kaneko K. Simulation study on the relationship between a high resolution α_S-plot and the pore size distribution for activated carbon. Carbon 1998; 36(10):1459-67.

[31] Wang ZM, Kanoh H, Kaneko K, Lu GQ, Do D. Structural and surface property changes of macadamia nut-shell char upon activation and high temperature treatment. Carbon 2002; 40(8): 1231-9.

[32] Stoeckli F, López-Ramon V, Moreno-Castilla C. Adsorption of phenolic compounds from aqueous solutions, by activated carbons, described by the Dubinin-Astakov equation. Langmuir 2001; 17(11): 3301-6.

[33] Stoeckli F, Hugi-Cleary D. On the mechanism of phenol adsorption by carbons. Russ Chem Bull Int Ed 2001; 50(11): 2060-3.

[34] Fernández E, Hugi-Cleary D, López-Ramón V, Stoeckli F. Adsorption of phenol from diluted and concentrated aqueous solutions by activated carbons. Langmuir 2003; 19(17): 9719-23.

[35] Murão PAM, Carrott PJM, Ribeiro Carrott MML. Application of different equations to adsorption isotherms of phenolic compounds on activated carbons prepared from cork. Carbon 2006; 44(12): 2422-9.

[36] Stoeckli F. In: Patrick J, editor. Porosity in carbons-characterization and applications. London: Arnold; 1995. p67-97.

[37] Stoeckli F. Dubinin's theory and its contribution to adsorption science. Russ Chem Bull Int Ed 2001; 50(12):2265-70.

[38] Carrott PJM, Ribeiro Carrott MML, Cansado IPP, Nabais JMV. Reference data for the adsorption of benzene on carbon materials. Carbon 2000; 38(3):465-74.

[39] Carrott PJM, Ribeiro Carrott MML, Cansado IPP. Reference data for the adsorption of dichloromethane on carbon materials. Carbon 2001; 39(3):465-72.

[40] Stoeckli F, López-Ramón V, Hugi-Cleary D, Guillot A. Micropore sizes in activated carbons determined from the Dubinin-Radushkevich equation. Carbon 2001; 39(7): 1115-6.

[41] Ohba T, Suzuki T, Kaneko K. Relation between DR-plot and micropore width distribution from GCMC simulation. Carbon 2000; 38(13):1892-6.

[42] Iso-15901: Pore size distribution and porosity of solid materials by mercury porosimetry and gas adsorption-Part 3: Analysis of micropores by gas adsorption.

[43] El-Merraoui M, Aoshima M, Kaneko K. Micropore size distribution of activated carbon fiber using the density functional theory and other methods. Langmuir 2000; 16(9): 4300-4.

[44] Bansal RC, Donnet JB, Stoeckli F. Active carbon. Marcel Dekker; New York 1988. p.158.

[45] Stoeckli F, Centeno TA. On the determination of surface areas in activated carbons. Carbon 2005; 43(6): 1184-90.

[46] Centeno TA, Sevilla M, Fuertes AB, Stoeckli F. On the lelctrical double layer capacitance of mesoporous templated carbons. Carbon 2005; 43 (14): 3012-5.

[47] Guillot A, Stoeckli F. Reference isotherm for high pressure adsorption of CO2 by carbons at 273 K. Carbon 2001; 39(13): 2059-64.

[48] Zubizarreta L, Gomez EI, Arenillas A, Ania CO, Parra JB, Pis JJ. H_2 storage in carbon materials. Adsorption 2008; 14: 557-66.

[49] Fernández JA, Morishita T, Toyoda M, Inagaki M, Stoeckli F, Centeno TA. Performance of mesoporous carbons derived from poly (vinyl alcohol) in electrochemical capacitors. J Power Sources 2008; 175(1): 675-9.

[50] Centeno TA, Fernandez JA, Kötz R, Stoeckli F. Correlation between capacitances of porous carbons in acidic and aprotic EDLC electrolytes. Electrochem Commun 2007; 9(6): 1242-6.

[51] Fernández JA, Arulepp M, Leis J, Stoeckli F, Centeno TA. EDLC performance of carbide-derived carbons in aprotic and acidic electrolytes. Electrochim Acta 2008; 53(24): 7111-6.

Fig. 1. Correlation between S_{BET} and V_{mi} for 190 activated carbons with pore widths between 0.5 and 1.8 nm (see Table 2).

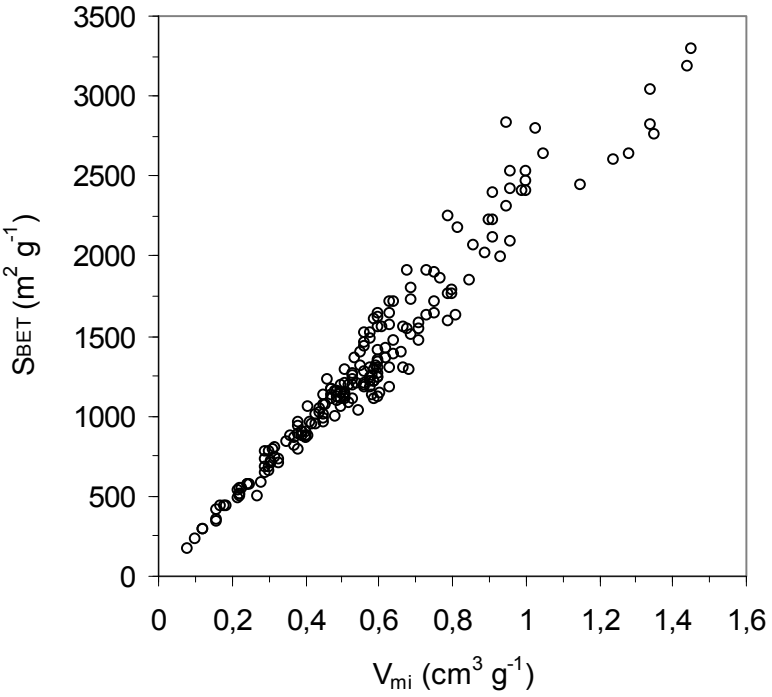

Fig. 2. Details for the correlation between S_{BET} and V_{mi} of CO_2 activated carbons fibers [22] (□), TiC-based carbon treated with H_2, or activated with KOH and CO_2 [28] (Δ) and a series of chemically and physically activated carbons [25] (◊). The insets correspond to the upper and lower pore sizes in the first two series (no data available for the third).

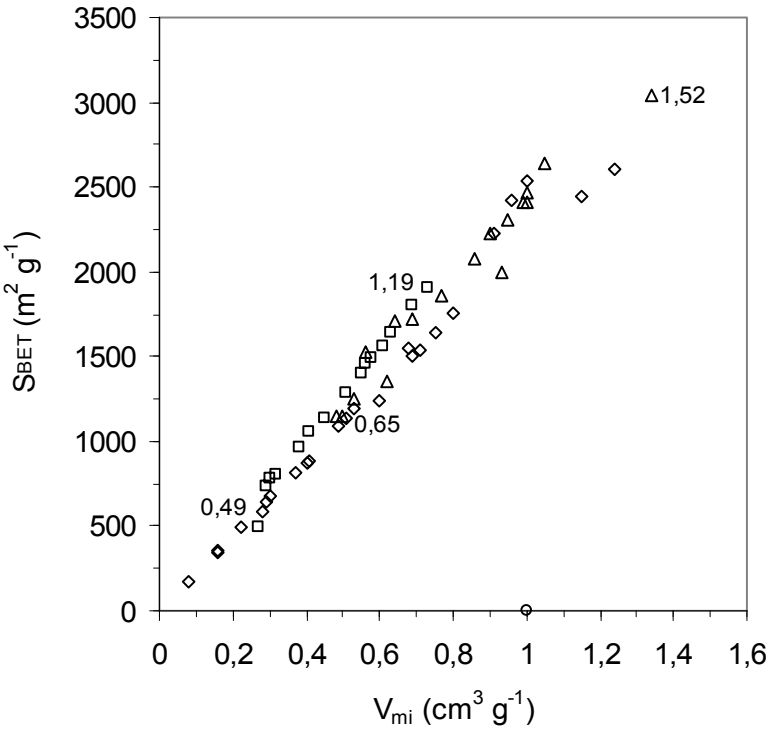

Fig. 3. Correlation between the enthalpy of immersion $\Delta_i H$(phenol 0.4M) and $S_{comp}(N_2$ 77 K) for 48 nano- and mesoporous carbons.

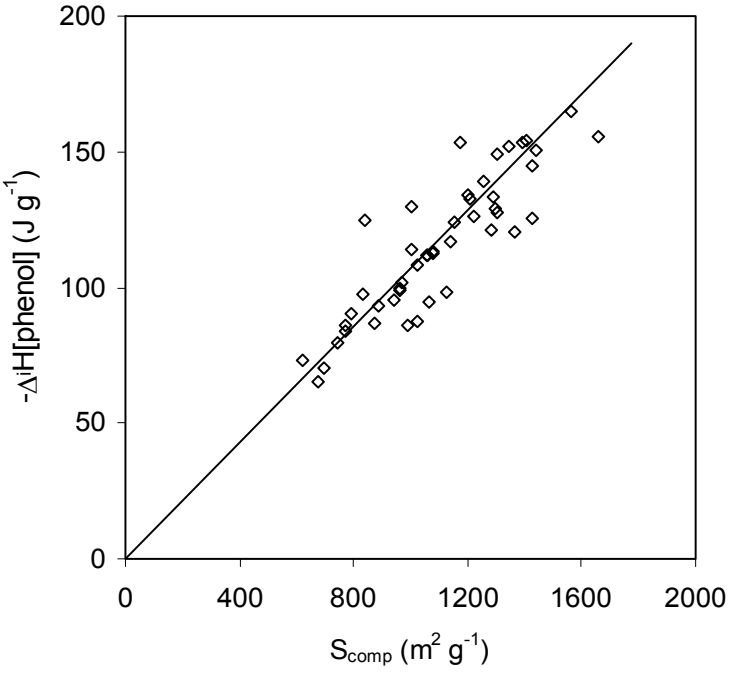

Fig. 4. Correlation between S_{tot}(DR; N_2 77 K) and S_{comp}(N_2 77 K) for 42 nanoporous carbons.

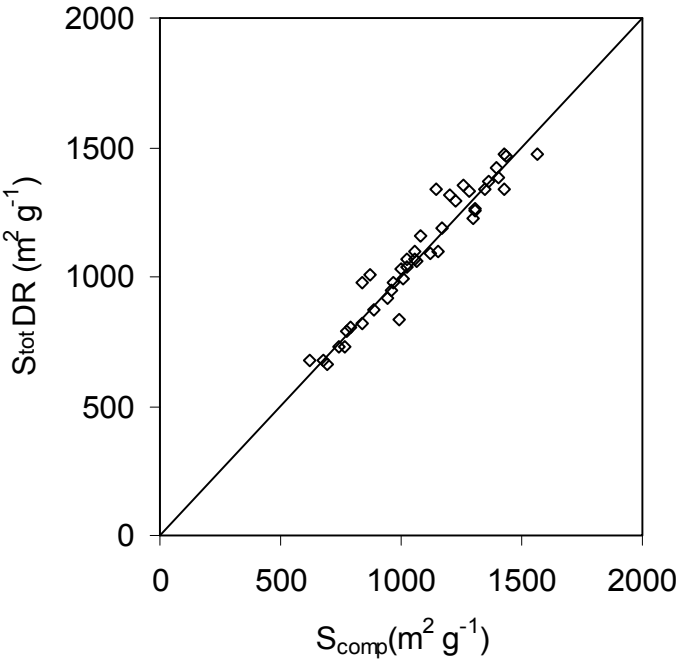

Fig. 5. Variation of $S_{BET}/S_{av}(3)$ (■) and $S_{BET}/S_{av}(4)$ (□) with the average pore width L_o for 42 nanoporous carbons. The average slopes are (1.20 ± 0.02) and (1.19 ± 0.03) nm^{-1}.

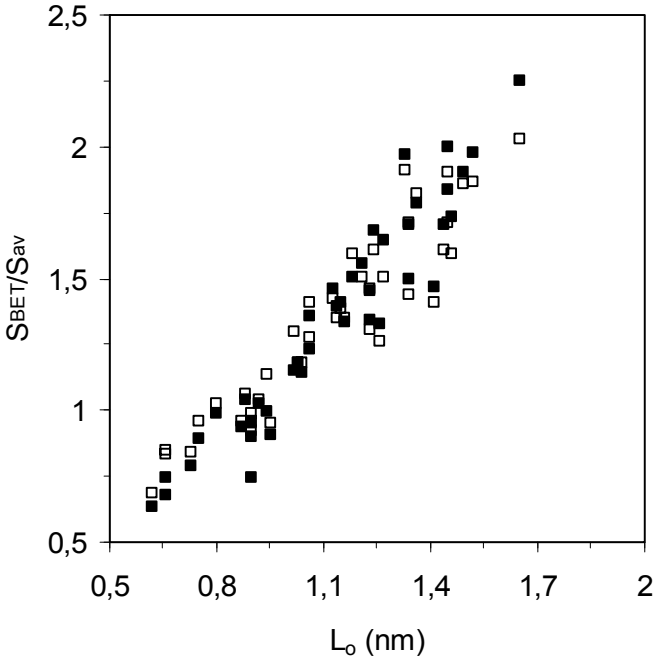

Table 1. Comparison of total surface areas for typical nanoporous carbons. The meaning of $S_{av}(3)$ and $S_{av}(4)$ is given in the text. The areas given below the carbon correspond to the average of all determinations, except S_{BET}

Carbon ($m^2\ g^{-1}$)	L_o (nm)	S_{comp} ($m^2\ g^{-1}$)	S_{phenol} ($m^2\ g^{-1}$)	S_{tot}(DR) ($m^2\ g^{-1}$)	S_{DFT} ($m^2\ g^{-1}$)	$S_{av}(3)$ ($m^2\ g^{-1}$)	$S_{av}(4)$ ($m^2\ g^{-1}$)	S_{BET} ($m^2\ g^{-1}$)
CMS-H2-07	0.81	619 (N_2)	697	678(N_2)	570	665	641	657
671± 51(8)		694(CH_2Cl_2)		719(CH_2Cl_2)				
		685 (C_6H_6)		710 (C_6H_6)				
DCG-5	1.15	888 (N_2)	885	869(N_2)	923	881	891	1238
903±66(6)		1023(C_6H_6)		830(C_6H_6)				
KF-1500-08	1.38	1055 (N_2)	1066	974(N_2)	1198	1032	1073	1652
1000±100(8)		946 (CO_2)		940 (CO_2)				
		982(C_6H_6)		870 (C_6H_6)				
N-125-08	1.60	768 (N_2)	821	732 (N_2)	958	773	820	1317
841±82(8)		811 (C_6H_6)		957 (C_6H_6)				
		846 (CCl_4)		847 (CCl_4)				

Table 2. Carbon series used for the linear correlations between BET-based areas and micropore volumes V_{mi} (see Figs. 1-2).

The uncertainties correspond to the standard deviations σ.

References	Origin of the carbons (number of samples)	S_{BET} $m^2\ g^{-1}$	V_{mi} $cm^3\ g^{-1}$	Pore width nm	S_{BET}/ V_{mi} $m^2\ cm^{-3}$	$(S_{BET}-S_e)/ V_{mi}$ $m^2\ cm^{-3}$
This work	Wood, anthracite, polymer, CDCs (42)	600-2800	0.3-1.0	0.66-1.65	2460 ± 40	2327 ± 60
	Activated apple char (16)	739-1604	0.39-0.59	0.87-1.19	2410 ± 40	2343 ± 110
	Phenolic resins (10)	710-1467	0.33-0.64	0.66-1.25	2230 ± 30	2134 ± 30
[19]	Steam-activated lignite and coal (9)	566-1110	0.24-0.52	1.02-1.84	2370 ± 110	2100 ± 160
[20, 21]	Polymer-based (12)	1102-1381	0.55-0.68	0.86-1.64	2410 ± 110	2200 ± 50
[13]	TiC-CDC 400-1000 ^oC (7)	1113-1623	0.51-0.81	0.68-1.10	2110 ± 50	-
[22]	CO_2 activated phenolic fibres (14)	499-1804	0.27-0.73	0.51-1.19	2560 ± 35	-
[23]	TiC-CDC 600-1000^oC +post-treatment (12)	1117-1381	0.59-0.68	0.86-1.64	1990 ± 140	-
[24]	VC-CDC 500-1100^oC (7)	236-1305	0.1-0.63	-	2270 ± 145	-
[25]	Anthracite, tar pitch, PAN fiber (24)	173-2602	0.08-1.24	-	2220 ± 120	-
[26]	PAN fibre HNO_3 treated 150-750^oC (6)	1173-1216	0.52-0.59	-	2080 ± 10	-
[27]	KOH activated Spanish anthracite (14)	726-3290	0.33-1.45	-	2190 ± 80	-
[28]	TiC-CDC treated with H_2, KOH, CO_2 (17)	1143-3038	0.48-1.34	0.65-1.52	2420 ± 150	-

Appendix A. Supplementary data

Table S1. BET analysis of the N_2 (77 K) adsorption isotherms of six microprous carbons. For carbons 2-5, see also Table 1 of the paper.

Carbon	Lo (nm)	S_{BET} (m^2 g^{-1})	V_M (cm^3 STP g^{-1})	c_{BET}	Relative Pressure Range
HK-650-8	0.66	759	174	35476	0.0009-0.081
CMS-H2-07	0.80	657	151	16282	0.0004-0.102
DCG-5	1.15	1238	284	1539	0.001-0.140
KF-1500-08	1.21	1652	380	1144	0.002-0.210
N-125-08	1.44	1317	311	848	0.005-0.210
PX-21	2.1	3214	738	72	0.049-0.216

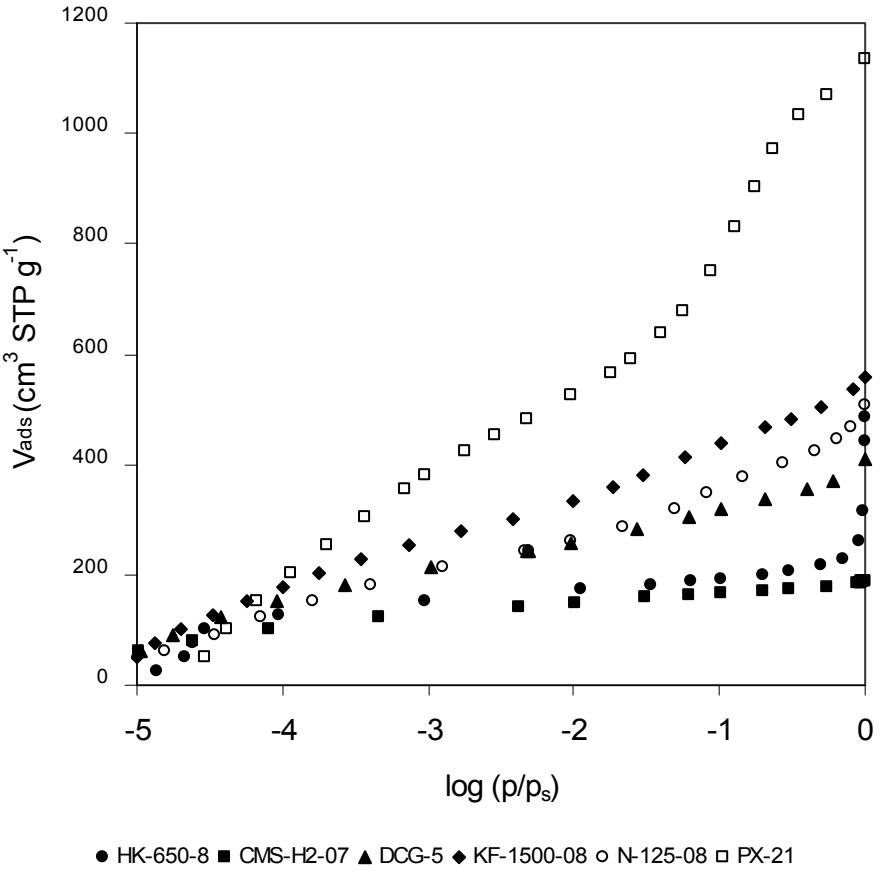

Fig. S1. Semi-logarithmic plots of the N_2 (77 K) isotherms of the six carbons.